ACS Catalysis

Research Article

pubs.acs.org/acscatalysis

# Role of Lewis and Brønsted Acidity in Metal Chloride Catalysis in Organic Media: Reductive Etherification of Furanics

Hannah Nguyen,[†] Nicholas Xiao,[†] Sean Daniels,[†] Nicholas Marcella,[‡] Janis Timoshenko,[‡] Anatoly Frenkel,[‡] and Dionisios G. Vlachos*[,†]

[†]Department of Chemical and Biomolecular Engineering, Catalysis Center for Energy Innovation, University of Delaware, 221 Academy Street, Newark, Delaware 19716, United States

[‡]Department of Material Science and Chemical Engineering, Stony Brook University, Stony Brook, New York 11794, United States

Supporting Information

**ABSTRACT:** Metal chlorides are demonstrated to behave as bifunctional acid catalysts in organic media in the one-pot reductive etherification of 5-hydroxymethylfurfural (HMF) in 2-propanol toward production of biodiesel. Two competing reaction pathways, direct etherification to 5-(isopropoxymethyl)furfural and reductive etherification to 2,5-bis-(isopropoxymethyl)furan, are proposed with the selectivity depending on the metal ion. Furfural and furfuryl alcohol are used as model compounds to investigate each pathway individually. The roles of Lewis/Brønsted acidity of metal chlorides solution are elucidated by kinetic studies in conjunction with salt speciation using electrospray soft ionization mass spectrometer. Brønsted acidic species, generated from alcoholysis of the metal chlorides, are the predominant catalytically active species in etherification. On the other hand, partially hydrolyzed metal cations produced by alcoholysis/hydrolysis are responsible Lewis acid centers for furfural reduction to furfuryl alcohol. Isotopic labeling experiments, in combination with GCMS and $^1$H NMR analysis, reveal an intermolecular hydrogen transfer from the $\alpha$-C of 2-propanol to the $\alpha$-C of furfural as the rate-limiting step of furfural hydrogenation.

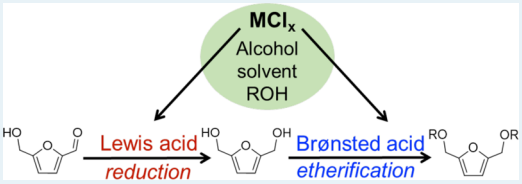


**KEYWORDS:** *reductive etherification, 5-hydroxymethyl furfural, furfuryl alcohol, furfural, metal chloride*

## INTRODUCTION

Research on renewable production of fuels has drawn significant attention due to rising concerns about climate change. Lignocellulosic biomass, the most natural abundant source of carbon, offers a green alternative to fuels without interfering with human-food consumption.[1] Biomass-derived furanyl ethers possess high cetane number, high energy density, and proven performance when blended with petroleum-derived diesel.[2,3] Such ethers can be synthesized from 5-hydroxymethyl furfural (HMF),[4] a biomass-derived platform chemical. HMF can be directly etherified by condensation with an alcohol to form 5-(alkoxymethyl)furfural (monoether),[5−7] or after hydrogenation of its carbonyl group followed by etherification to form 2,5-bis(alkoxymethyl)furan (diether), i.e., a reductive etherification route.[3,8,9] The diether is higher grade fuel than the monoether owing to its higher stability and miscibility with commercial diesel.[3,9] While acid-catalyzed etherification of HMF to a monoether with ion exchange resins,[3,10,11] heteropolyacids,[12] aluminosilicates,[7,13] mineral acid,[3,13] and metal salts[14−18] as catalysts has been studied quite extensively, literature on synthesis of the diether is limited. Bell and co-workers reported up to 60% yield to diether in a cascade reaction under $H_2$ pressure using a physical mixture of Pt/$Al_2O_3$ and Amberlyst-15.[3] More recently, Jae et al. and Lewis et al. independently investigated the use of metal-substituted BEA zeolites for the one-pot synthesis of the diether in 2-propanol or ethanol, without $H_2$ gas.[8,9] In this route, the Lewis acids are hypothesized to facilitate catalytic transfer hydrogenation of HMF by the Meerwein−Ponndorf−Verley (MPV) reduction in alcohol solvent that is also acting as a hydrogen donor. The product of the MPV reduction is sequentially etherified to the maximum of ca. 80% diether yield.[8,9] Diether formation was also reported over metal oxide catalysts.[19,20] Evidently, reductive etherification of HMF is a promising process for production of diether on account of several advantages: single catalyst, no $H_2$ gas required, and one-pot reactor for process efficiency.

Besides metal-substituted BEA zeolites, whose synthesis is still rather challenging, conventional homogeneous Lewis acid metal chlorides (e.g., $CrCl_3$, $AlCl_3$) have been shown to be effective for intramolecular MPV reduction of aldose to ketose (e.g., glucose isomerization).[21−26] Mechanistic studies have revealed that the active-site structures of Sn-BEA and metal chlorides share striking similarities and facilitate the same catalytic pathways in aqueous solution.[22,23,27−31] In the chelated transition state, characteristic of MPV reduction, the metal center coordinates the O1 and O2 atoms of the aldose (e.g., glucose) during an intramolecular hydride shift from the C2 to

Received: July 16, 2017
Revised: September 13, 2017
Published: September 15, 2017




DOI: 10.1021/acscatal.7b02348
ACS Catal. 2017, 7, 7363−7370

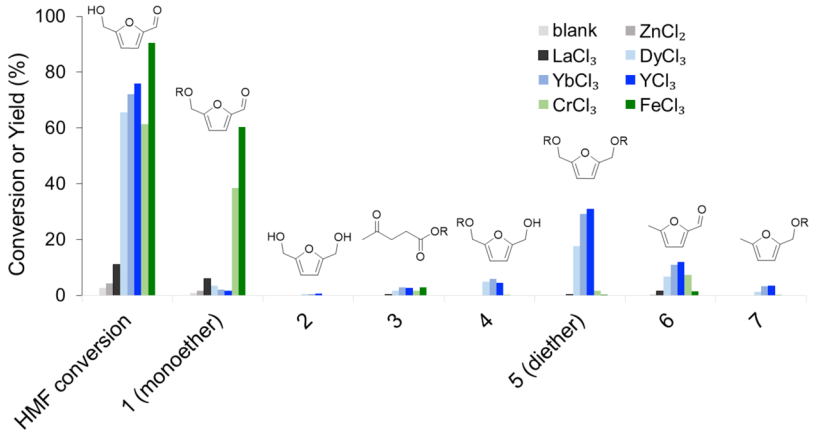


**Figure 1.** HMF conversion and product yields in 2-propanol catalyzed by variety of metal chlorides. Reaction conditions: 1 wt % HMF, 3 mM catalyst, 150 °C, 1 h reaction time. R represents an isopropyl group.

the C1 carbon. Because of the analogies between zeolites and metal salts for isomerization of glucose, one might speculate on the potential activity of metal salts for reductive etherification of HMF. In addition, metal salts offer promising reusability as they are shown to be effectively recyclable after multiple runs without significant activity loss for glucose isomerization/dehydration to HMF.[32,33]

Although metal salts have been demonstrated to be effective catalysts for direct etherification of HMF to monoether in alcohol solvent,[14−16] no diether production has been reported. Our group previously investigated catalysis of furfural hydrogenolysis by metal chlorides in 2-propanol, and we have observed formation of isopropyl furfuryl ether.[34] However, that work focused on synthesis of methyl furan and did not further explore the potential for reductive etherification.

Herein, we assess the catalytic activity of inexpensive, conventional Lewis acid metal chlorides for the tandem reductive etherification of HMF in 2-propanol, and reveal two main reaction pathways, depending on the metal cation. Furfuryl alcohol (FA) and furfural are employed as model compounds to further investigate each of the two pathways independently. By correlating the metal chloride speciation and reaction kinetics, we demonstrate that the metal chlorides actually play a bifunctional role in the reductive etherification of furanic compounds in organic media.

## EXPERIMENTAL METHODS

**Materials.** All chemicals and solvents were purchased from Sigma-Aldrich and used without further modification. Reactants are HMF, furfural, and FA. The catalysts include $ZnCl_2$, $CrCl_3.6H_2O$, $FeCl_3.6H_2O$, $YbCl_3.6H_2O$, $DyCl_3.6H_2O$, $LaCl_3.7H_2O$, and $YCl_3.6H_2O$ as well as 0.1 M HCl in 2-propanol. Deuterated solvents for isotopic labeling experiments are 2-propanol-d8 ($(CD_3)_2CDOD$) and 2-propanol-OD ($(CH_3)_2CHOD$).

**Reductive Etherification Experiments.** A typical experiment was carried out in a 100 mL Parr reactor vessel, consisting of 70 mL of 2-propanol solution of a metal salt and the reactant (HMF or furfural), sealed with 20 bar $N_2$. The reactor was heated to the desired temperature in a customized band heater, using a temperature controller. Samples were taken periodically and filtered for post-reaction analysis.

**Etherification Kinetic Experiments.** Kinetic study of FA reactions was conducted in 5 mL thick walled glass vials, consisting of 2 mL of 2-propanol solution of 1 wt % FA and 5−20 mM catalyst ($CrCl_3$, $YCl_3$ or HCl). The reactor vials were heated to 90 °C, in a temperature-controlled-aluminum block on a magnetic stir plate, and quenched in an ice bath at desired time points. The small glass reactors were used, instead of a Parr reactor, to provide better data for the reaction kinetic model because they require minimal heating time. This setup can only be used at low temperatures ($T \leq 120$ °C)

**Product Analysis.** Products were identified with a gas chromatogram-mass spectrometer (GC-MS) system (Shimadzu QP 2010 Plus). Except for HMF, all quantifications were done in a GC (Agilent 7890 A), equipped with a HP-INNOWAX column, a flame ionization detector (FID), and a quantitative carbon detector (Polyarc). The Polyarc reactor converts organic compounds to methane and gives a universal response in the FID to eliminate cumbersome calibrations.[35] Product concentrations were determined using the calibration curve for FA and carbon numbers of the product molecules. The method was verified by the collapse of calibration curves for various organic compounds with different carbon numbers (Figure S1). HMF quantification was carried out with an Agilent 1200 Series high performance liquid chromatography (HPLC), equipped with a C-18 column (Agilent).

**pH Measurement.** The pH of the solutions was measured with a glass pH electrode (Mettler Toledo InLab Science) and an Acumic basic AB 15 pH meter.

**Spectroscopy Techniques.** Electrospray soft ionization mass spectra (ESI-MS) of the metal chloride solutions in 2-propanol were collected with a single quadrupole mass spectrometer (SQD2), using 2-propanol as mobile phase with the following parameters: capillary voltage 2.8 kV, extractor voltage 5 V, sample cone voltage, 20 V, source temperature, 363 K, desolvation temperature, 423 K, cone gas ($N_2$) flow, 40 L/h. X-ray absorption measurement (XAS) were performed at Cr K-edge ($Z$ = 24, $E_0$ = 5989 eV) in fluorescence mode, and Y K-edge ($Z$ = 39, $E_0$ = 17 038 eV) in transmission mode at Stanford Synchrotron Radiation Lightsource. Nuclear magnetic resonance $^1$H NMR spectra of the post reaction solutions were recorded using a Bruker 400 MHz NMR spectrometer.

## RESULTS AND DISCUSSION

**Catalytic Activity of Metal Chlorides for Reductive Etherification of HMF.** Various metal chlorides ($MCl_x$) were screened for HMF reaction in 2-propanol and exhibited a wide



DOI: 10.1021/acscatal.7b02348
ACS Catal. 2017, 7, 7363−7370

**Scheme 1. Proposed Reaction Network of HMF Reactions by $MCl_3$ in 2-Propanol**[a]

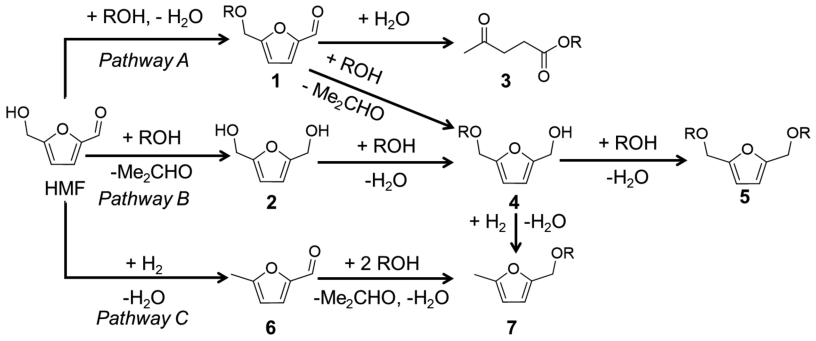


[a]OR = $OCH(CH_3)_2$.

range of catalytic activity under the same reaction conditions (Figure 1). While $ZnCl_2$ and $LaCl_3$ showed little activity, other salts gave more than 60% HMF conversion. In all the experiments, low HMF initial concentration of 1 wt % was used to minimize self-condensation of HMF to heavy products[9] and enable focus on the mechanism of the main reactions. GCMS analysis revealed various products such as 5-(isopropoxymethyl)furfural **1** (monoether), 2,5-bis(hydroxymethyl)furan **2**, isopropyl levulinate **3**, 5-isopropoxymethylfurfuryl alcohol **4**, 2,5-bis(isopropoxymethyl)furan **5** (diether), 5-methyl furfural **6**, and 2-(isopropoxymethyl) 5-methyl furan **7**. The observed products are similar to those of HMF reactions over Lewis acid zeolites (e.g., Sn-BEA) in alcohol solvents.[8,9] We postulate a reaction network of HMF reaction in 2-propanol solution of $MCl_x$, consisting of three major pathways (Scheme 1). In pathway A, HMF etherification with 2-propanol forms **1**, which undergoes hydrolytic ring-opening to **3**. Pathway B proceeds via HMF transfer hydrogenation to **2**, followed by etherification to **4** and **5**. In pathway C, hydrogenolysis of HMF produces **6**, which is further reduced and etherified to **7**. Formation of hydrogenolysis products was also reported with solid Lewis acid Sn-BEA, presumably realized by in situ $H_2$ generation and use.[9] Further investigation of the hydrogenolysis pathway is outside the scope of this work.

Among the tested catalysts, $YCl_3$ exhibited the highest activity for reductive etherification with approximately 35% yield to diether **5** without reaction-condition optimization. $DyCl_3$ and $YbCl_3$ also produced **5** as the major product at slightly lower yields. The post-reaction solutions turned dark brown due to significant polymerization. Nevertheless, our results demonstrate that some metal chlorides can be potential catalysts for one-pot reductive etherification of HMF to the diether. Noticeably, the product distribution significantly depends on the metal. While $YCl_3$, $YbCl_3$, and $DyCl_3$ favor reaction pathway B to the diether as stated, $CrCl_3$ and $FeCl_3$ selectively facilitate the direct etherification pathway A with up to 60% yield of the monoether **1**. The differences in activity and selectivity of $MCl_3$ for each pathway suggest the involvement of multiple catalytically active species and reaction mechanisms.

To untangle this complex reaction system, we used model compounds in order to study each reaction pathway independently: FA for direct etherification (pathway A); and furfural for reductive etherification (pathway B). $CrCl_3$ and $YCl_3$ were chosen as representative catalysts on account of their demonstrated chemoselectivity.

**Furfuryl Alcohol (FA) Etherification.** *Reaction Network.* First, we investigate the direct etherification of FA. Mirroring the reactivity trend of HMF reaction (pathway A), $CrCl_3$ is significantly more active than $YCl_3$, yielding 3.5 times as much ether (Figure S2). The low pH values of the 10 mM $MCl_3$ solutions (1.23 for $CrCl_3$ and 1.91 for $YCl_3$) indicates that the solutions are acidic, likely due to protons released from $MCl_3$ alcoholysis.

$$MCl_x + (n+m)(ROH) \leftrightarrow MCl_{(x-n)}(OR)_n \cdot (ROH)_m + nHCl \quad \text{(R1)}$$

Multiple studies have attributed the activity of metal salts in FA reactions to their induced Brønsted acidity; the FA conversion and product yields qualitatively correlate with pH of the salt solution.[36,37] However, the pH measurement in alcohol solvent does not provide the true acid concentration because it largely depends on the solvent.[38] Our attempts to experimentally measure the induced HCl concentration by acid−base titration were unsuccessful, possibly due to the base interference with the $MCl_3$ speciation. Moreover, measurements at room temperature to quantify the Hammett acidity do not reflect the true induced Brønsted acidity at elevated temperatures. Thus, a quantitative relationship between the reactivity of metal salts and the induced Brønsted acidity has yet to be established. In addition, the catalytic role of the Lewis acidic metal chloride species itself remains elusive.

To deconvolute the Lewis and induced Brønsted acid contributions of $MCl_3$ solutions, herein we develop a simple reaction kinetic model of FA reaction in 2-propanol starting with the product speciation. Aside from isopropyl furfuryl ether (iPFE), isopropyl levulinate (iPL) was identified as another major product, which is also a value-added chemical, reported to form via FA alcoholysis.[11,36,37,39−41] Traces of 2-chloromethyl furan, $\alpha$-angelica lactone, and dimerization products of furfuryl alcohol were observed in GC/GCMS analysis. The post reaction solutions turned yellowish, probably due to FA polymerization. A typical time-dependent concentration profile shows that iPFE and iPL initially form in parallel, consistent with the published work on FA alcoholysis in ethanol by Maldonado and co-workers.[11] The authors also suggested that the two minor pathways to ethyl levulinate are through ethyl furfuryl ether and 4,5,5-triethoxypentan-2-one (TEP) as intermediates. However, the corresponding 2-propanol analogue of TEP, 4,5,5-tri-isopropoxy-pentan-2-one (TIPP), was not observed in the course of our reactions. Interestingly, when ethanol or 1-propanol was used as the solvent, at the same reaction conditions, the corresponding trialkoxypentan-2-ones were detected as major products



DOI: 10.1021/acscatal.7b02348
ACS Catal. 2017, 7, 7363−7370

(Figure S3). The absence of TIPP suggests that the compound may not be stable in 2-propanol. As a result, we propose a FA reaction network, whereby iPL could form either directly from FA or via the iPFE intermediate (Scheme 2, blue arrows).

**Scheme 2. Proposed Reaction Network of Furfural Reductive Etherification in 2-Propanol[a]**

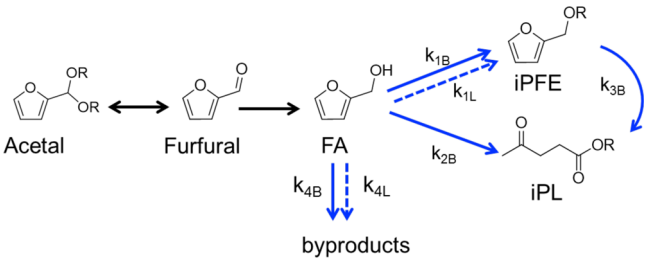


[a]Furfuryl alcohol reaction network in blue arrows.

To assess to role of induced Brønsted acidity, experiments were performed with HCl in the absence of $MCl_3$. Comparison of the selectivity for iPL and iPFE among $CrCl_3$, $YCl_3$, and HCl suggests that the FA reactions are not solely Brønsted acid-catalyzed. The iPFE to iPL ratios for $YCl_3$ and $CrCl_3$ were higher than that for HCl, at the same FA conversion, indicating that FA etherification by $MCl_3$ was slightly more favored (Figure 2). Barbera et al. reported formation of furfuryl ether

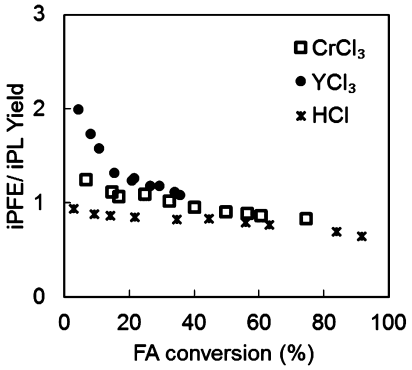


**Figure 2.** Selectivity to isopropyl furfuryl ether (iPFE) over isopropy levulinate (iPL) in $CrCl_3$, $YCl_3$, and HCl. Reaction conditions: 1 wt % furfuryl alcohol, 90 °C, 10 mM catalyst.

with either $ZrO_2$ (containing only Lewis acid sites) or sulfated $ZrO_2$ (containing both Lewis and Brønsted acid sites). Levulinate, on the other hand, was only observed in the presence of Brønsted acids (namely, after sulfation).[42] These important findings have been incorporated into our reaction network, where now FA etherification and side reactions can be facilitated by either the Lewis acid, $MCl_3$, or the induced Brønsted acid, HCl; while iPL formation pathways are catalyzed by HCl only (Scheme 2, blue arrows).

*Kinetic Model.* Using the proposed reaction network, we developed a simple kinetic model to assess the intrinsic catalytic activity of $MCl_3$ solutions. Due to the lack of in situ experimental methods to determine the acidity of $MCl_3$ solutions, the induced [HCl] was assumed to be a linear function of $[MCl_3]$ within a rather small catalyst-concentration range (5−10 mM). (From the speciation equilibrium, one should expect a quadratic-like relationship between [HCl] and $[MCl_3]$, which can be approximated as linear within a small range.) The assumed linearity is consistent with the linear correlation between $[MCl_3]$ and [HCl] in aqueous solution predicted by the thermodynamic model OLI for various metal salts under similar reaction conditions (Figure S4; the OLI model has been validated in past work.[21,43]) The kinetic model assumes a perfectly mixed batch reactor and first-order dependence on the reactant and acid centers, as follows:

$$\frac{dC_{FA}}{dt} = -((k_{1B} + k_{2B} + k_{4B})[HCl] + (k_{1L} + k_{4L})[MCl_3])C_{FA}$$

$$\frac{dC_{iPFE}}{dt} = (k_{1B}[HCl] + k_{1L}[MCl_3])C_{FA} - k_{3B}[HCl]C_{iPFE}$$

$$\frac{dC_{iPL}}{dt} = k_{2B}[HCl]C_{FA} + k_{3B}[HCl]C_{iPFE}$$

$$\frac{dC_{byproducts}}{dt} = (k_{4B}[HCl] + k_{4L}[MCl_3])C_{FA}$$

$$\text{induced acidity, } [HCl] = a[MCl_3] + b$$

where $k_{iB}$ is the rate constant of the $i^{th}$ Brønsted acid-catalyzed reaction (blue solid arrows, Scheme 2); $k_{iL}$ is the rate constant of the $i^{th}$ Lewis acid-catalyzed reaction (blue dashed arrows, Scheme 2); and $a$ and $b$ describe the induced [HCl]. The model parameters were regressed to the experimental concentration profiles of FA, iPFE, iPL, and byproducts (determined by carbon balance) using the *lsqnonlin* nonlinear fitting function in Matlab. The regression procedure was similar to that used in our earlier work on the tandem isomerization/dehydration of glucose by $CrCl_3$.[43] Specifically, the model rate constants were fitted in two stages. First, we fitted the rate constants of the reactions catalyzed by HCl alone (Table 1). Then, we fitted the kinetic model for $MCl_3$, including the parameters $a$ and $b$ (Table 1).

Representative transient profiles of FA and of the products show good agreement between the model and the experimental data (Figure 3). Comparison of the rate constants reveals that the Brønsted acid is substantially more effective for FA etherification than the Lewis acid metal species, with $k_{1B}$ being 18-fold and 60-fold higher than $k_{1L}$ for $CrCl_3$ and $YCl_3$, respectively. A similar trend is observed for the side reactions. The superior reactivity of Brønsted acids for etherification has

**Table 1. Predicted Rate Constants of Furfuryl Alcohol (FA) Reactions in Scheme 2[a]**

| Brønsted acid-catalyzed rate constant $k_B$ ($M^{-1}min^{-1}$) | | | | Lewis acid-catalyzed rate constant $k_L$ ($M^{-1}min^{-1}$) | | | | induced $[HCl] = a[MCl_3] + b$ | | | |
|---|---|---|---|---|---|---|---|---|---|---|---|
| | | | | $CrCl_3$ | | $YCl_3$ | | $CrCl_3$ | | $YCl_3$ | |
| $k_{1B}$ | $k_{2B}$ | $k_{3B}$ | $k_{4B}$ | $k_{1L}$ | $k_{4L}$ | $k_{1L}$ | $k_{4L}$ | $a$ | $b$ | $a$ | $b$ |
| 0.34 | 0.38 | 0.11 | 0.07 | 0.019 | $3.4 \times 10^{-3}$ | $5.6 \times 10^{-3}$ | $5.3 \times 10^{-4}$ | 0.235 | $8.1 \times 10^{-4}$ | 0.0264 | $1.7 \times 10^{-4}$ |

[a]Reaction conditions: 1 wt % FA, 90 °C, 5−10 mM $MCl_3$, 5−20 mM HCl.



DOI: 10.1021/acscatal.7b02348
ACS Catal. 2017, 7, 7363−7370

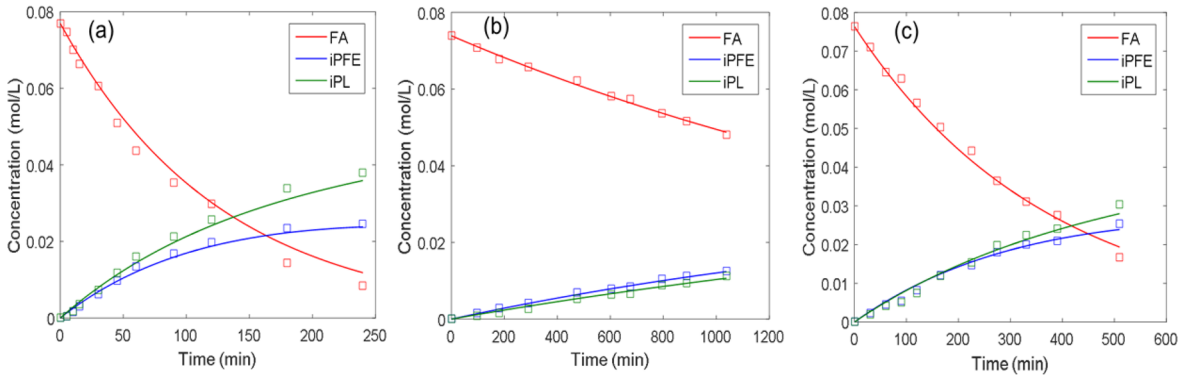


**Figure 3.** Experimental (symbols) and modeling (lines) concentration profiles of furfuryl alcohol (FA), isorpropyl furfuryl ether (iPFE) and isopropyl levulinate (iPL) in HCl (a), $YCl_3$ (b) and $CrCl_3$ (c). Reaction conditions: 1 wt % FA, 10 mM catalyst, 90 °C.

also been observed for solid acid catalysts. For example, Barbera et al. showed significant enhancement of ether formation after $ZrO_2$ sulfation.[42] Recently, Schwartz and co-workers reported orders of magnitude higher rates for etherification by Brønsted acids (H-zeolites) than Lewis acids ($\gamma$-$Al_2O_3$).[44] Additionally, our model predicts that the concentration of induced HCl in $CrCl_3$ solution is nearly an order of magnitude higher than in $YCl_3$ solution (Figure S5). That is rationalized from the fact that Cr(III) is a stronger Lewis acid, making it easier for a solvated alcohol to lose a proton (alcoholyze) and produce a more acidic solution, similar to hydrolysis of the metal aqua cations.[45] Apparent rate constants ($k_{1app}$) were also determined to quantitate the overall observed reactivity (Figure 4). Clearly,

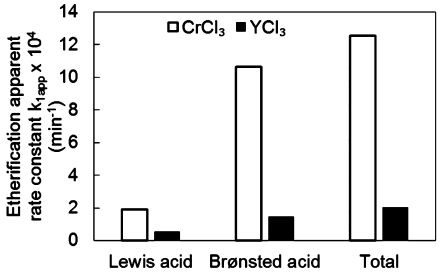


**Figure 4.** Apparent rate constant of furfuryl alcohol etherification $k_{1app} = k_1$[catalyst] of 10 mM $CrCl_3$ and $YCl_3$.

*FA etherification by $MCl_3$ is primarily governed by the induced Brønsted acidity instead of the Lewis acidity.* Even though $CrCl_3$ is a more effective Lewis acid for etherification (higher $k_{1L}$) than $YCl_3$, the substantially higher ether formation-rate observed for $CrCl_3$ is mostly attributed to the higher concentration of induced HCl.

**Furfural Reduction.** *Reaction Mechanism.* Furfural was employed to study the reduction pathway B, Scheme 1. Isotopic tracing experiments in deuterated 2-propanol, in combination with GCMS analysis were carried out to investigate the furfural reduction mechanism by $YCl_3$ (Figure 5) and $CrCl_3$ (Figure S6). When 2-propanol solvent is unlabeled (2-propanol-d0), the GCMS fragmentation of the FA product is the same as the FA standard, with the parent ion $m/z$ = 98. However, in 2-propanol-d8 ($(CD_3)_2CDOD$) solvent, the parent ion of the FA product is $m/z$ = 99. A unit shift in the spectrum of FA produced in 2-propanol-d8 indicates that one of the H atoms in the molecule has been replaced by a D, supportive of an intermolecular hydrogen transfer mechanism from 2-propanol to furfural. To examine the possibility of a dihydride

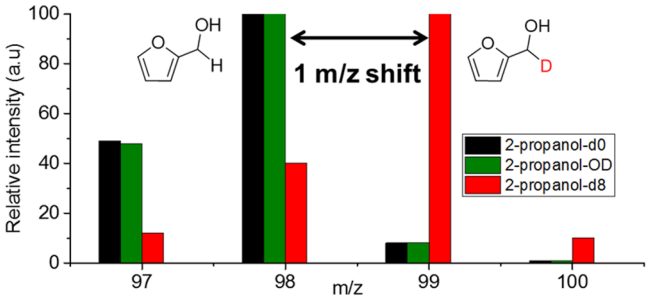


**Figure 5.** GCMS spectra of furfuryl alcohol product. Reaction conditions: 1 wt % furfural, 150 °C, 3 mM $YCl_3$, in 2-propanol-d0 ($t$ = 30 min), 2-propanol-OD ($t$ = 30 min), and 2-propanol-d8 ($t$ = 1 h).

mechanism, which usually occurs when catalysis involves a metal hydride,[46] 2-propanol-OD ($(CH_3)_2CHOD$)) was used as the solvent. The GCMS closely resembles that in 2-propanol-d0, suggesting that there was no H scrambling between O of 2-propanol and $\alpha$-C of furfural. Consequently, we inferred that both $CrCl_3$ and $YCl_3$ facilitate furfural reduction via *an intermolecular hydrogen transfer (MPV) from $\alpha$-C of 2-propanol to $\alpha$-C of furfural.*

$^1$H NMR spectra of the post reaction mixtures in $YCl_3$ further support this conclusion by revealing the location of the replacing D (Figure 6). All three spectra in 2-propanol-d0, 2-propanol-OD and 2-propanol-d8 display the four distinguished peaks of FA at around 7.4 ppm ($H_a$), 6.32 ppm ($H_b$), 6.27 ppm ($H_c$) and 4.54 ppm ($H_d$), where the first three peaks are assigned to the three H atoms on the furan ring, and the last peak belongs to H at $\alpha$-C. The integrated peak ratio $H_d$: $H_c$ is equal to 2:1, corresponding to the relative number of H giving rise to the resonances, in standard FA, and FA product in 2-propanol-d0 and 2-propanol-OD. However, in the $^1$H NMR spectrum in 2-propanol-d8, the $H_d$: $H_c$ peak ratio is 1:1, indicating that one of the H atoms at the $\alpha$-C was replaced by D. Primary kinetic isotope effect ($k_H/k_D$ = 2.22) was observed when a 1:1 by volume mixture of 2-propanol-d0 and 2-propanol-d8 was used as solvent, corresponding to $H_d$:$H_c$ ratio of 1.31. Attempts to carry out the same $^1$H NMR study for $CrCl_3$ were unsuccessful due to the paramagnetic nature of Cr, broadening the peaks and causing peak integration difficult. However, a mixture of unlabeled and labeled FA was observed in the GCMS of FA produced in 1:1 mixture of 2-propanol by $CrCl_3$, resembling that by $YCl_3$ and suggesting a similar kinetic isotope effect (Figure S7). Therefore, the intermolecular hydrogen transfer from $\alpha$-C of 2-propanol to $\alpha$-C of furfural


DOI: 10.1021/acscatal.7b02348
ACS Catal. 2017, 7, 7363−7370

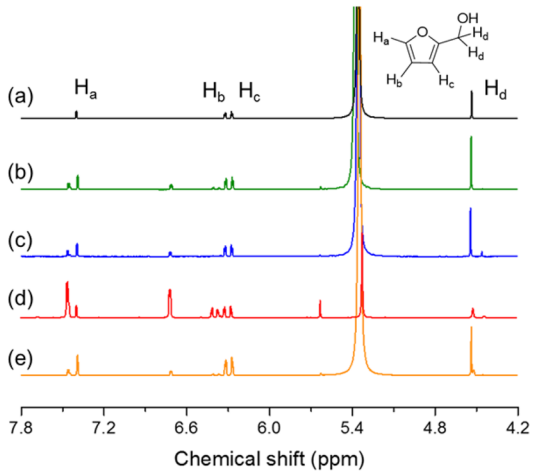


**Figure 6.** $^1$H NMR spectra of furfuryl alcohol standard (a) and post reaction mixture of furfural reduction by $YCl_3$ in 2-propanol-d0 (b), 2-propanol-OD (c), 2-propanol-d8 (d), and 1:1 mixture of 2-propanol-d0 and 2-propanol-d8 (e).

is likely the rate-determining step for furfural reduction by $MCl_3$.

*Determination of Catalytically Active Species.* Besides FA, identifiable products in GC/GCMS analysis include iPFE and iPL, as well as trace amounts of the aldol condensation product of furfural and acetone. Noticeably, 2-furaldehyde di-isopropyl acetal was detected instantaneously after furfural and the catalyst solution were mixed, and decreased over the course of the reaction. It suggests that acetalization of furfural and 2-propanol is a fast and reversible reaction, pointing to the overall reaction network in Scheme 2. Similarly to the observed activity trend for HMF, furfural reduction is considerably more favorable in $YCl_3$, with nearly 10-fold higher FA yield than in $CrCl_3$ at the same reaction conditions (Figure S8). Given the lower Brønsted acidity of $YCl_3$ solutions compared with $CrCl_3$ solutions, the higher $YCl_3$ reactivity for furfural reduction indicates that the reaction is catalyzed by Lewis acid metal species.

Alcoholysis of a metal chloride in 2-propanol forms metal isopropoxide cations, which are highly sensitive to moisture and may be hydrolyzed in the presence of water[47,48] in the $MCl_3.6H_2O$ solution. The alcoholyzed/hydrolyzed metal ions may also condense to form metal clusters.[49] The various metal species have been detected in ESI-MS and XAS of $MCl_3$ solution in 2-propanol (see Figure S9 and Table S1 for more details). Consequently, $MCl_3$ speciation is hypothesized to proceed via the following generalized steps of alcoholysis (R1), hydrolysis (R2), and oligomerization (R3):

$$MCl_{(x-n)}(OR)_n\cdot(ROH)_m + nH_2O \leftrightarrow MCl_{(x-n)}(OH)_n\cdot(ROH)_m + n\mathrm{ROH} \quad \text{(R2)}$$

$$MCl_{(x-n)}(OH)_n + MCl_{(x-m)}(OH)_m \rightarrow M_2Cl_{(2x-n-m)}(OH)_{(n+m-2)}O + H_2O \quad \text{(R3)}$$

The various metal complexes may possess different catalytic properties toward the reduction of furfural. Our previous studies on glucose isomerization by $MCl_3$ in aqueous solutions revealed $M(OH)^{2+}$ as the active species.[21,22] Adding excess HCl suppresses the hydrolyzed species, resulting in a drop of reactivity.[21] In a similar vein, here we investigated how adding HCl to $MCl_3$ solutions would influence activity toward furfural reduction. In the case of $YCl_3$, the furfural conversion and product yields drop monotonically with increasing [HCl] (Figure 7a). Interestingly, the $CrCl_3$ activity exhibits a maximum at increasing HCl concentration before dropping (Figure 7b). HCl partly prevents alcoholysis/hydrolysis of $MCl_3$ (R1 and R2), i.e., the formation of partially hydrolyzed metal cations. Because $CrCl_3$ is much more likely to be alcoholyzed/hydrolyzed than $YCl_3$, it is possible that hydrolyzed metal cations oligomerize (R3) due to their higher concentrations, thereby, reaching a maximum at an optimum [HCl]. Thus, we infer that the catalytically active species for furfural reduction are partially hydrolyzed metal cations. Computational studies of the mechanism of glucose isomerization by $CrCl_3$ have shown that the basic hydroxyl ligand on the metal center is essential, as it accepts a proton from the hydroxyl group at C2 carbon of glucose, which activates the intramolecular C2−C1 hydride shift at the Lewis acid metal center.[26] An analogous synergy might be drawn here for transfer hydrogenation of furfural. Overall, $CrCl_3$ and $YCl_3$ were shown to facilitate furfural reduction via the same intermolecular hydrogen transfer mechanism and have similar active species.

Experiments with varying temperature were conducted to determine the activation energy for furfural reduction by $MCl_3$. The rate constants were calculated using the initial-rate

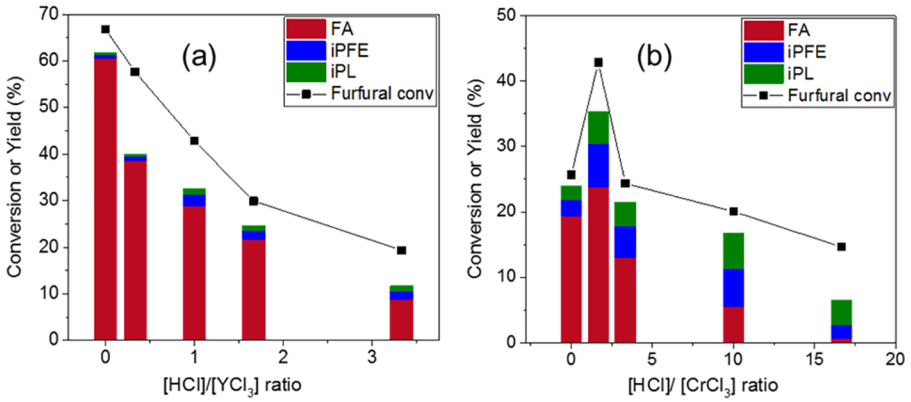


**Figure 7.** Effect of HCl addition on furfural conversion and product yields by $YCl_3$ (a) and $CrCl_3$ (b). Reaction conditions: 1 wt % furfural, 150 °C, 3 mM $MCl_3$, $t$ = 30 min ($YCl_3$), $t$ = 180 min ($CrCl_3$).



DOI: 10.1021/acscatal.7b02348
ACS Catal. 2017, 7, 7363−7370

approach, specifically from the initially linear part of the time-dependent profile of the total amount of product formation (FA, iPFE, iPL). A lower apparent activation energy was found for $CrCl_3$ than for $YCl_3$ (25.6 vs 30 kcal/mol) despite its lower rate (see Arrhenius plots in Figure S10). It should be noted that since the active species forms in situ through metal salt alcoholysis/hydrolysis, its concentration is dependent on temperature. The higher apparent activation energy of $YCl_3$ could potentially be due to more hydrolyzed metal cations formation at higher temperatures. The intrinsic reactivity of $CrCl_3$ and $YCl_3$ should only be compared at the same active species concentration, which is currently challenging to determine at reaction temperatures.

## CONCLUSIONS

We have evaluated the catalytic activity of various metal chlorides for the tandem reductive etherification of HMF in 2-propanol. Two main parallel reaction pathways were identified: direct etherification to monoether, favored by $CrCl_3$ and $FeCl_3$ (pathway A), and reductive etherification to diether, preferred by $YCl_3$, $YbCl_3$, and $DyCl_3$ (pathway B). To isolate each pathway, we employed model compounds: FA for pathway A and furfural for pathway B, with $CrCl_3$ and $YCl_3$ as representative catalysts. Through modeling of kinetic experiments, we quantified for the first-time contributions from the Lewis acid metal species and from the induced Brønsted acidity, HCl, for FA etherification. The turnover frequency for etherification of FA by HCl is an order of magnitude higher than that by $MCl_3$, suggesting that the etherification activity over metal chlorides is governed by the induced Brønsted acidity. $CrCl_3$ favors etherification over $YCl_3$ owing to its higher ability to alcoholyze and produce protons. On the other hand, furfural reduction (hydrogenation) is facilitated by Lewis acidic species. We carried out isotopic labeling experiments to investigate the mechanism of furfural reduction. GCMS and $^1$H NMR analysis revealed that intermolecular hydrogen transfer from the $\alpha$-C of 2-propanol to the $\alpha$-C of furfural is the rate-determining step. On the basis of the correlation between the effect of HCl addition on the speciation of metal salts and on the $MCl_3$ activity for furfural reduction, we hypothesized that the catalytic active species for the transfer hydrogenation is a partially hydrolyzed metal cation, similar to the active species in glucose isomerization by $MCl_3$ in aqueous solution. The mechanistic understanding and methodology introduced in this work could provide insights into Lewis and Brønsted acid catalysis in organic media for other reactions.

## ASSOCIATED CONTENT

### Supporting Information

The Supporting Information is available free of charge on the ACS Publications website at DOI: 10.1021/acscatal.7b02348.

Additional experimental details, figures, tables, and references (PDF)

## AUTHOR INFORMATION


### Corresponding Author

*E-mail: vlachos@udel.edu.

### ORCID

Anatoly Frenkel: 0000-0002-5451-1207

Dionisios G. Vlachos: 0000-0002-6795-8403


### Notes

The authors declare no competing financial interest.

## ACKNOWLEDGMENTS

This work was supported as part of the Catalysis Center for Energy Innovation, an Energy Frontier Research Center funded by the US Dept. of Energy, Office of Science, Office of Basic Energy Sciences under award number DE-SC0001004. The ESI-MS instrument was supported by the National Institute of General Medical Sciences of the National Institutes of Health under Award Number P20GM104316; the content is solely the responsibility of the authors and does not necessarily represent the official views of the NIH. The authors would like to thank Dr. Stavros Caratzoulas and Prof. Raul Lobo for useful discussions.

## REFERENCES


(1) Corma, A.; Iborra, S.; Velty, A. *Chem. Rev.* **2007**, *107*, 2411−2502.

(2) Mascal, M.; Nikitin, E. B. *Angew. Chem., Int. Ed.* **2008**, *47*, 7924−6.

(3) Balakrishnan, M.; Sacia, E. R.; Bell, A. T. *Green Chem.* **2012**, *14*, 1626.

(4) Bohre, A.; Dutta, S.; Saha, B.; Abu-Omar, M. M. *ACS Sustainable Chem. Eng.* **2015**, *3*, 1263−1277.

(5) Raveendra, G.; Rajasekhar, A.; Srinivas, M.; Sai Prasad, P. S.; Lingaiah, N. *Appl. Catal., A* **2016**, *520*, 105−113.

(6) Che, P.; Lu, F.; Zhang, J.; Huang, Y.; Nie, X.; Gao, J.; Xu, J. *Bioresour. Technol.* **2012**, *119*, 433−6.

(7) Lanzafame, P.; Temi, D. M.; Perathoner, S.; Centi, G.; Macario, A.; Aloise, A.; Giordano, G. *Catal. Today* **2011**, *175*, 435−441.

(8) Lewis, J. D.; Van de Vyver, S.; Crisci, A. J.; Gunther, W. R.; Michaelis, V. K.; Griffin, R. G.; Roman-Leshkov, Y. *ChemSusChem* **2014**, *7*, 2255−65.

(9) Jae, J.; Mahmoud, E.; Lobo, R. F.; Vlachos, D. G. *ChemCatChem* **2014**, *6*, 508−513.

(10) Sacia, E. R.; Balakrishnan, M.; Bell, A. T. *J. Catal.* **2014**, *313*, 70−79.

(11) Gonzalez Maldonado, G. M.; Assary, R. S.; Dumesic, J.; Curtiss, L. A. *Energy Environ. Sci.* **2012**, *5*, 8990−8997.

(12) Wang, H.; Deng, T.; Wang, Y.; Qi, Y.; Hou, X.; Zhu, Y. *Bioresour. Technol.* **2013**, *136*, 394−400.

(13) Arias, K. S.; Climent, M. J.; Corma, A.; Iborra, S. *ChemSusChem* **2014**, *7*, 210−20.

(14) Jia, X.; Ma, J.; Che, P.; Lu, F.; Miao, H.; Gao, J.; Xu, J. *J. Energy Chem.* **2013**, *22*, 93−97.

(15) Zhou, X.; Zhang, Z.; Liu, B.; Zhou, Q.; Wang, S.; Deng, K. *J. Ind. Eng. Chem.* **2014**, *20*, 644−649.

(16) Dutta, S.; De, S.; Alam, M. I.; Abu-Omar, M. M.; Saha, B. *J. Catal.* **2012**, *288*, 8−15.

(17) Liu, B.; Zhang, Z.; Huang, K.; Fang, Z. *Fuel* **2013**, *113*, 625−631.

(18) Liu, J.; Tang, Y.; Wu, K.; Bi, C.; Cui, Q. *Carbohydr. Res.* **2012**, *350*, 20−4.

(19) Hao, W.; Li, W.; Tang, X.; Zeng, X.; Sun, Y.; Liu, S.; Lin, L. *Green Chem.* **2016**, *18*, 1080−1088.

(20) Luo, J.; Yu, J.; Gorte, R. J.; Mahmoud, E.; Vlachos, D. G.; Smith, M. A. *Catal. Sci. Technol.* **2014**, *4*, 3074−3081.

(21) Choudhary, V.; Mushrif, S. H.; Ho, C.; Anderko, A.; Nikolakis, V.; Marinkovic, N. S.; Frenkel, A. I.; Sandler, S. I.; Vlachos, D. G. *J. Am. Chem. Soc.* **2013**, *135*, 3997−4006.

(22) Choudhary, V.; Pinar, A. B.; Lobo, R. F.; Vlachos, D. G.; Sandler, S. I. *ChemSusChem* **2013**, *6*, 2369−76.

(23) Tang, J.; Guo, X.; Zhu, L.; Hu, C. *ACS Catal.* **2015**, *5*, 5097−5103.

(24) Pagán-Torres, Y. J.; Wang, T.; Gallo, J. M. R.; Shanks, B. H.; Dumesic, J. A. *ACS Catal.* **2012**, *2*, 930−934.

(25) Wang, T.; Pagán-Torres, Y. J.; Combs, E. J.; Dumesic, J. A.; Shanks, B. H. *Top. Catal.* **2012**, *55*, 657−662.
(26) Mushrif, S. H.; Varghese, J. J.; Vlachos, D. G. *Phys. Chem. Chem. Phys.* **2014**, *16*, 19564−19572.
(27) Nguyen, H.; Nikolakis, V.; Vlachos, D. G. *ACS Catal.* **2016**, *6*, 1497−1504.
(28) Bermejo-Deval, R.; Orazov, M.; Gounder, R.; Hwang, S.-J.; Davis, M. E. *ACS Catal.* **2014**, *4*, 2288−2297.
(29) Moliner, M.; Román-Leshkov, Y.; Davis, M. E. *Proc. Natl. Acad. Sci. U. S. A.* **2010**, *107*, 6164−6168.
(30) Román-Leshkov, Y.; Moliner, M.; Labinger, J. A.; Davis, M. E. *Angew. Chem., Int. Ed.* **2010**, *49*, 8954−8957.
(31) Bermejo-Deval, R.; Assary, R. S.; Nikolla, E.; Moliner, M.; Román-Leshkov, Y.; Hwang, S.-J.; Palsdottir, A.; Silverman, D.; Lobo, R. F.; Curtiss, L. A.; Davis, M. E. *Proc. Natl. Acad. Sci. U. S. A.* **2012**, *109*, 9727−9732.
(32) Wang, T.; Pagán-Torres, Y. J.; Combs, E. J.; Dumesic, J. A.; Shanks, B. H. *Top. Catal.* **2012**, *55*, 657−662.
(33) Roy Goswami, S.; Dumont, M.-J.; Raghavan, V. *Ind. Eng. Chem. Res.* **2016**, *55*, 4473−4481.
(34) Panagiotopoulou, P.; Martin, N.; Vlachos, D. G. *ChemSusChem* **2015**, *8*, 2046−54.
(35) Beach, C. A.; Krumm, C.; Spanjers, C. S.; Maduskar, S.; Jones, A. J.; Dauenhauer, P. J. *Analyst* **2016**, *141*, 1627−32.
(36) Huang, Y.-B.; Yang, T.; Zhou, M.-C.; Pan, H.; Fu, Y. *Green Chem.* **2016**, *18*, 1516−1523.
(37) Peng, L.; Gao, X.; Chen, K. *Fuel* **2015**, *160*, 123−131.
(38) A guide to pH measurement-the theory and practice of laboratory pH applications. http://www.mt.com/us/en/home/library/guides/lab-analytical-instruments/pH-Theory-Guide.html (accessed Feb 27, 2017).
(39) Enumula, S. S.; Koppadi, K. S.; Babu Gurram, V. R.; Burri, D. R.; Rao Kamaraju, S. R. *Sustainable Energy Fuels.* **2017**, *1*, 644−651.
(40) Zhang, Z.; Dong, K.; Zhao, Z. K. *ChemSusChem* **2011**, *4*, 112−8.
(41) Démolis, A.; Essayem, N.; Rataboul, F. *ACS Sustainable Chem. Eng.* **2014**, *2*, 1338−1352.
(42) Barbera, K.; Lanzafame, P.; Pistone, A.; Millesi, S.; Malandrino, G.; Gulino, A.; Perathoner, S.; Centi, G. *J. Catal.* **2015**, *323*, 19−32.
(43) Dallas Swift, T.; Nguyen, H.; Anderko, A.; Nikolakis, V.; Vlachos, D. G. *Green Chem.* **2015**, *17*, 4725−4735.
(44) Meredith, C.; Allen, W. G.; Schwartz, T. J. Functionalization of 5-hydroxymethylfurfural by selective etherification. *25th North American Catalysis Society Meeting*, Denver, CO, June 4−9, 2017.
(45) Richens, D. *The chemistry of aqua ions: synthesis, structure, and reactivity: a tour through the periodic table of the elements*; John Wiley & Sons: Hoboken, NJ, 1997; pp 44−55.
(46) Samec, J. S. M.; Backvall, J.-E.; Andersson, P. G.; Brandt, P. *Chem. Soc. Rev.* **2006**, *35*, 237−248.
(47) Bradley, D. C.; Mehrotra, R. C.; Rothwell, I. P.; Singh, A. *Alkoxo and Aryloxo Derivatives of Metals*; Academic Press: London, 2001; pp 3−181.
(48) *The Chemistry of Metal Alkoxides*; Turova, N. Y., Turevskaya, E. P., Kessler, V. G., Yanovskaya, M. I., Eds.; Springer US: Boston, MA, 2002; pp 11−30.
(49) Rahaman, M. N. *Ceramic Processing and Sintering*. Taylor & Francis: NewYork, 2003; pp 260−277.



DOI: 10.1021/acscatal.7b02348
*ACS Catal.* 2017, 7, 7363−7370